

Vestibular coriolis effect differences modeled with three-dimensional linear-angular interactions

Jan E. Holly

Department of Mathematics, Colby College, Mayflower Hill Drive, Waterville, ME 04901, USA
Tel.: +1 207 872 3202; Fax: +1 207 872 3801; E-mail: jeholly@colby.edu

Accepted 6 August 2004

Abstract. The vestibular coriolis (or “cross-coupling”) effect is traditionally explained by cross-coupled angular vectors, which, however, do not explain the differences in perceptual disturbance under different acceleration conditions. For example, during head roll tilt in a rotating chair, the magnitude of perceptual disturbance is affected by a number of factors, including acceleration or deceleration of the chair rotation or a zero-g environment. Therefore, it has been suggested that linear-angular interactions play a role.

The present research investigated whether these perceptual differences and others involving linear coriolis accelerations could be explained under one common framework: the laws of motion in three dimensions, which include all linear-angular interactions among all six components of motion (three angular and three linear).

The results show that the three-dimensional laws of motion predict the differences in perceptual disturbance. No special properties of the vestibular system or nervous system are required. In addition, simulations were performed with angular, linear, and tilt time constants inserted into the model, giving the same predictions. Three-dimensional graphics were used to highlight the manner in which linear-angular interaction causes perceptual disturbance, and a crucial component is the Stretch Factor, which measures the “unexpected” linear component.

Keywords: Perception, motion sickness, zero-g, cross-coupling, self-motion

1. Introduction

We as humans know from practical experience that linear and rotational cues are combined in our perception of self-motion to form a three-dimensional impression of motion. Furthermore, experimental evidence shows that three-dimensional linear and angular information are combined physiologically, for example in post-rotatory eye-movement responses that reorient, even in the dark, depending on the changed direction of the linear gravity vector after head tilt [1, 42,44]. Linear-angular combination is also confirmed at the level of central neurons, many of which receive both linear and angular input [4,11,12,49,53].

1.1. The vestibular coriolis/cross-coupling effect

Linear-angular interaction is called upon to explain certain experimental results on the vestibular coriolis (or “cross-coupling”) effect, though the basic explanation of the vestibular cross-coupling effect involves only angular vectors: If a subject in the dark is being rotated counterclockwise at constant velocity, for instance, then a rightward head roll is associated with an angular acceleration in the forward pitch direction which may be perceived as a disorienting forward tumble (Fig. 1). The effect can be modeled as due to cross-coupling of angular velocity vectors; the direction and magnitude of the angular acceleration are given by the cross product between the (yaw) angular velocity of the rotating reference frame of the subject and the (roll) an-

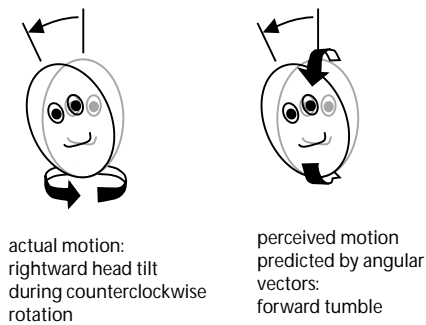


Fig. 1. Classic vestibular coriolis (or “cross-coupling”) effect, demonstrated with counterclockwise rotation and rightward head roll. Analysis of angular vectors alone gives a prediction from angular cross-coupling of perceived forward tumble with a head-yaw rotation component.

angular velocity of the head within the rotating reference frame. Although such cross-coupling occurs regardless of the type of angular acceleration sensor, the vestibular literature typically gives an intuitive description of the physics by considering sensors at steady-state prior to head tilt, and discussing the acceleration effects in the semicircular-canal planes or idealizations of them [21, 23,38]. In the end, the explanation is straight from the laws of motion—an angular acceleration arises from two angular velocities.

Vestibular cross-coupling is typically used to explain the disorientation experienced by subjects upon head tilt during rotation in the dark, but cross-coupling is insufficient to explain the differences in magnitude of disorientation under different acceleration conditions. Even during head tilt causing identical magnitudes of cross-coupled vectors, an accelerating rotation of the chair results in a smaller magnitude of perceptual disturbance than does a constant-velocity rotation of the chair, while a decelerating rotation of the chair results in a larger magnitude of perceptual disturbance than does a constant-velocity rotation [23]. In addition, disturbances are significantly less during cross-coupling experiments in zero-g, both in subjects who have lived in zero-g for days [19,20] and in subjects who are in a zero-g environment for less than a minute [36].

A linear vector—the gravity vector—is called upon to help explain the differences in magnitude of disturbance in the different environments. For the accelerating-rotation condition the direction of the gravity vector is consistent with the perceived angular velocity (about an earth-vertical axis), while in the decelerating-rotation condition the gravity and perceived angular velocity vectors are incompatible because the gravity vector does not rotate in conjunction with the perceived

angular velocity (about a non-vertical axis) [5,23,57]. A greater mismatch thus correlates with a greater perceptual disturbance. For the differences in perceptual effect between the 1 g and zero-g conditions, explanations involve reduced responsiveness to semicircular canal activity and/or muscle activation patterns that are dependent upon the direction of the linear gravity vector in 1 g but not in zero-g [13,35,36].

The linear coriolis force, also, is involved if the head is tilted away from the axis of rotation. Upon such tilt, a linear acceleration of the head occurs in a direction tangential to the now-off-axis circular motion of the head, in order to start the head moving around the circle. Technically, the linear coriolis “force” is an apparent force opposing this increasing circular motion; the magnitude of the head’s acceleration is equal to (though technically oppositely-directed from) the “linear coriolis acceleration”. This acceleration of the head occurs throughout the tilt, and just like the cross-coupled vector, would be expected to have effects lasting past the time of the tilt because there is no concluding reverse acceleration to stop any induced perception of motion.

However, despite the apparent significance of the gravitational linear vector for perceptual disturbance, an increase in magnitude of perceptual disturbance, measured in terms of motion sickness, was not found with an increase in magnitude of the linear coriolis vectors in experiments testing the importance of the linear coriolis vector [32]. Instead, the magnitude of disturbance was found to be correlated with the speed of rotation [32,33].

At first glance, the non-correlation (and possibly even negative correlation [32]) of disturbance with linear coriolis force seems contradictory to the idea that disturbance is greater with a larger linear (1 g versus 0 g) vector. After all, the linear coriolis vector is, just like the gravity vector, incompatible with the perceived angular velocity vector. At a second glance, it is clear that the motions are complex enough to require a more thorough three-dimensional investigation that covers the various acceleration environments as well as different amounts of tilt away from the rotation axis in 1 g.

1.2. Laws of motion

The first explanation for motion-perception phenomena is typically the external laws of physics, i.e. the laws of motion. Often, a perception can be explained by relating the accelerations directly by the laws of motion to perceived velocities and orientation. Sometimes

a second step must be taken by appealing to special properties of the nervous system to explain observed deviations from what the laws of motion would suggest.

A basic example of a laws-of-motion explanation is that used for the false perception, in the dark, of rotation after decelerating to a stop from a period of constant-velocity on-axis rotation. The explanation requires use of (1) the subject's "initial"—i.e. preceding the deceleration—perception of motion, and (2) the accelerations imposed on the subject during the deceleration. A subject's initial perception—during sustained constant-velocity, say counterclockwise, rotation—is typically of being stationary (because no angular acceleration impinges on the subject, and the vestibular system has equilibrated). Then during deceleration, a clockwise acceleration is imposed upon the subject to stop the rotation. By the laws of motion, a clockwise acceleration imposed upon an initially stationary object will cause the object to rotate clockwise, so it is not surprising that subjects typically report a (false) perception of rotating clockwise. The subjects' nervous systems are simply doing their jobs; a perfect processor of acceleration information would give the same report of rotation, assuming that it is initialized to match the subjects' initial perception.

In this rotation example, the basic perception is explained by the laws of motion. Over the long term, however, subjects' perceptions of rotation slowly decay, a decay that would not be reported by a perfect processor of acceleration information. Therefore, time constants of decay of rotation perception are measured experimentally for subjects, and are a special property of the nervous system (with explanations related to biological noise), used to complete the long-term explanation of this perception of self-motion. It is worth noting that the decay of rotation perception need not be considered "caused by" the fluid dynamics and the biomechanics of the sensors, but may be considered a phenomenon of the perceptual system as a whole. In fact, the dynamics of the sensors would not, in general, impede a perfect processor's abilities as long as the processor took into account the sensor dynamics in response to the external stimulus, acceleration. In particular, a perfect processor of acceleration information could appropriately maintain a perception of velocity after acceleration ends. Indeed, the nervous system does perform this maintenance of velocity perception, at least for a time, after sensor movement has decayed [22]. The sensor-afferent-central nervous system linkage can, therefore, be considered as a whole when comparing the physiological system with a perfect processor of acceleration information.

Another example of a laws-of-motion explanation is the standard explanation, above, of the vestibular cross-coupling effect. This explanation, as well, requires use of (1) subjects' initial—prior to head tilt—perception of motion, and (2) accelerations imposed on the subject during the head tilt.

The laws of motion in three dimensions explain more complex phenomena as well. For example, an investigation [29] using the full three-dimensional laws of motion explains the faster change in tilt perception during deceleration than during acceleration in a fixed-carriage centrifuge [10,18]. In other words, the physics of the motion itself predicts the perceptual tilt-change asymmetry, without addition of parameters for a physiological system as included in other models predicting perceptual tilt-change asymmetry [8,16,17,39,40,43,52,59]. Further comparison with other models is included in the Discussion. Another three-dimensional investigation [30] explains acceleration-deceleration differences, including tumbling sensations during deceleration, in a centrifuge whose carriage tilts during the run [24]. In addition, the laws of motion in three dimensions explain [31] clockwise-counterclockwise differences in perceptual effects from head turn while supine in a rotating centrifuge [26].

1.3. *Linear-angular interaction in the vestibular coriolis/cross-coupling effect*

The goal of the present paper is to determine whether the observed differences in vestibular coriolis/cross-coupling effects can be explained by the laws of motion in three-dimensions. This investigation requires the use of all six degrees of freedom (three angular and three linear) and all linear-angular interactions in three dimensions. The goal is to mirror the standard physics explanation of the vestibular cross-coupling effect, but to include both linear and angular accelerations, and to display the resulting predicted (by the laws of motion) perceived motion in a three-dimensional format [29–31]. In order to accomplish this full display, the computations must keep track of not only perceived velocities and direction of gravity, but also the location and the three-dimensional orientation relative to the starting position. From the three-dimensional displays of predicted perceived motion in the different conditions, the results will be compared between conditions by means of two measures of possible disorientation: the Twist Factor and the Stretch Factor, representing the angular discrepancy and the linear displacement, respectively, between the actual head tilt relative to the body and the

three-dimensional motion that is predicted to be perceived instead. The question is whether the laws of motion, as manifest in the Twist and Stretch Factors extracted from the three-dimensional displays, explain the differences in magnitude of perceptual disturbance in the different conditions. A secondary goal is to carry out the same test with a model that implements the laws of motion but processed with time constants, as are often used in vestibular models to mirror experimentally-observed physiological time constants.

2. Methods

Two sets of motions were investigated. Used throughout was rightward head roll of 30° in 1 sec (Fig. 2) with a sinusoidal velocity profile during counterclockwise “chair” rotation. The first set of motions had rightward head roll on-axis, with counterclockwise chair rotation of 1 rad/s. The four different conditions were:

STANDARD: During constant-velocity chair rotation of 1 rad/s, the head rolled to the right.

ACCELERATING: The chair rotation was accelerating at 0.26 rad/s^2 . When the velocity reached 1 rad/s, the head rolled to the right (while the chair acceleration continued).

DECELERATING: The chair rotation was decelerating at 0.26 rad/s^2 . When the velocity reached 1 rad/s, the head rolled to the right (while the chair deceleration continued).

MICROGRAVITY: During chair rotation of 1 rad/s in a zero-g environment, the head rolled to the right.

The second set of motions used head roll that moved off-axis, i.e. away from the vertical axis of rotation. A comparison was made between different roll radii and different rotation speeds. The three conditions were:

SHORT&SLOW: During constant-velocity chair rotation of 1 rad/s, the head rolled to the right with a 0.1 m radius of rightward roll (so that the head moved away from the vertical axis).

LONG&SLOW: During constant-velocity rotation of 1 rad/s, the head rolled to the right with a 0.2 m radius (twice “SHORT”) of rightward roll.

SHORT&FAST: During constant-velocity chair rotation of 2 rad/s (twice “SLOW”), the head rolled to the right with a 0.1 m radius of rightward roll.

Additional testing was done for “neck lengths” (roll radii) in the range 0.1 m to 0.7 m, and for chair rotation speeds in the range 1 rad/s to 7 rad/s.

2.1. Three-dimensional computations: Perfect processor

For each motion, a simulation was carried out to compute the three-dimensional perception over a two second period (one second during head roll plus one second following head roll, with the head in 30° rightward-roll orientation) that would be predicted by the laws of motion in three dimensions. In other words, this is the perception that would be reported by a perfect processor of acceleration information whose initial perceptual conditions—just prior to the head roll—matched those of a typical experimental subject. In the computations for the MICROGRAVITY condition, the fact that gravity was absent was known (and felt) by the perfect processor. The accelerations were considered to be detected at a single point, so that centripetal acceleration during on-axis rotation did not give a perception of rotation, just as it does not in human subjects. These computations were analogous to, and extended, standard analyses of the vestibular cross-coupling/coriolis effect. For example, a perfect processor that begins with a perception of no rotation (as does a subject) and then has rightward head roll within a rotating environment will report forward pitch because of cross-coupled angular velocities. The present computations, however, extended the standard analyses by including all six degrees of freedom (three angular and three linear) as well as all linear-angular interactions, including those due to the presence of gravity, and by displaying the results of the linear-angular interactions in a three-dimensional format.

The results of computations were displayed in a three-dimensional format showing the simulated perception by the perfect processor, of the head motion relative to the body. The actual head motion relative to the body is rightward roll in every condition.

2.2. Twist and stretch factors: Perfect processor

Two measures were developed for comparing the different conditions’ three-dimensional results. These two measures gave the total angular and linear deviation of the computed perception as compared to the actual rightward head roll relative to the body. In other words, the measures gave the deviation in perception from the actual motion. This deviation could also be viewed as an internal conflict, because the computed perception is based upon acceleration sensors, while the actual motion relative to the body is detected by neck proprioceptive sensors.

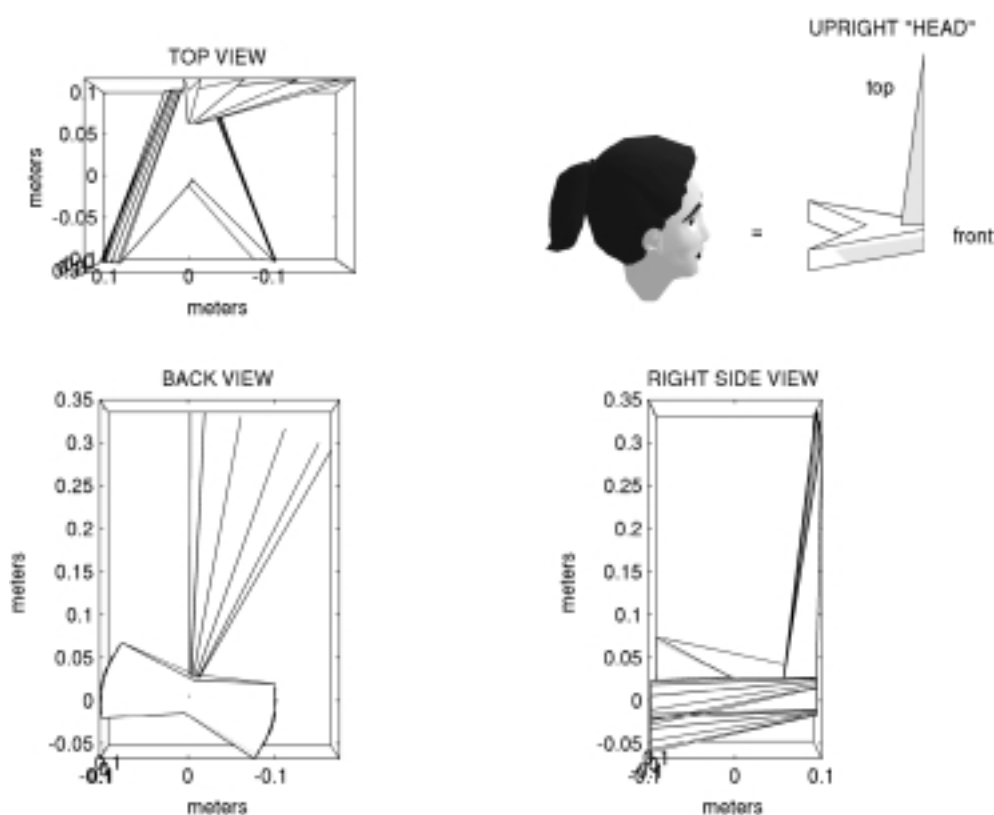


Fig. 2. The polyhedron used to display head position and orientation in three dimensions, and the basic rightward head roll. Upper right shows the polyhedron along with the head that it represents, indicating the meaning of the polyhedron in the figures throughout the paper. This polyhedron with clear angular features is used in order to facilitate the three-dimensional display of orientation. The other three panels show a time-lapse picture of the actual 30° rightward head roll relative to the body. A snapshot is shown of the polyhedral "head" every 0.2 s, from 0 to 1 s.

The measure of angular deviation, the Twist Factor, was the accumulated angle through which the perceived head motion proceeded differently from the actual roll motion. The Twist Factor was calculated by first computing at each point in time the three-dimensional orientation of the perceived motion *relative to* the actual roll motion. Next computed was the angle through which this orientation rotated in three dimensions from one time step to the next; time steps of 0.1 s were used. The Twist Factor at each point in time was then calculated as the sum of these "deviant" rotation angles up to that time. For example, if the perceived motion were simply the roll motion, then the three-dimensional relative orientation would have been a constant "zero" orientation, and therefore, it would have rotated through no angle over time, and the Twist Factor would have been zero for all time.

The measure of linear deviation, the Stretch Factor, was the accumulated distance that the perceived head motion proceeded differently from the actual motion. Actual linear head motion relative to the body

was zero in conditions STANDARD, ACCELERATING, DECELERATING, and MICROGRAVITY, and was nonzero for the other conditions, in which the head made an arc. The Stretch Factor was computed by integrating using a time step of 0.1 s.

Twist and Stretch Factors were computed during the same two seconds as used in the three-dimensional simulations, starting with the one second of head roll and continuing for one more second after head-roll velocity had stopped. Additional testing up to ten seconds always followed the trend of the first two seconds.

2.3. Three-dimensional computations: With time constants

A second set of simulations also used a laws-of-motion-based processor of three-dimensional acceleration information, but which included time constants for decay of rotation perception, for decay of linear motion perception, and for tilt so that the subjective vertical approached alignment with the gravito-inertial accel-

ation (GIA, the detected linear acceleration, which is the sum of the linear acceleration and, in the 1g simulations, the earth-upward 1g vector that is indistinguishable from linear acceleration by Einstein's Equivalence Principle). Values used were 20 s for angular, 0.5 s for linear, and 5 s for tilt based upon experimental studies, e.g. [25,46,54,55] and discussed further in the Discussion; different values would not be expected to affect the results of the present research because the present goals are *to compare* predicted perceived motions, and all such motions are affected similarly by the time constants. In fact, the inclusion of time constants, at all, would not be expected to change the results, for the same reason and because the motions' time frame is short. However, time constants are a well-known property of perception.

2.4. Twist and stretch factors: With time constants

For the simulations with time constants, Twist and Stretch Factors were computed in the same way as for the perfect-processor simulations, with one change. The comparison "actual" motion was a time-constant rightward head roll. In other words, the comparison movement of rightward head roll was modified slightly so that an actual rightward head roll while *not rotating* would give values of zero for the Twist and Stretch Factors, reflecting no perceptual disturbance.

2.5. Equations

For the computations, head-coincident coordinates [28] were used, in which velocities and accelerations are given in a coordinate system coincident with the head but temporarily fixed relative to the earth in order to specify any non-zero linear or angular velocity of the head. In other words, the velocity of the head at any given point in time is specified by using a coordinate system coincident with the head's, but fixed relative to the earth, and specifying head velocity in that fixed system. This type of coordinate system mirrors a subject's viewpoint in which the subject's own sensors are always oriented with the subject. The standard orientation of head axes [27] was used, with the positive x -axis pointing noseward, y -axis pointing leftward, and z -axis pointing head-upward. This head-coincident coordinate system was used in conjunction with an earth-fixed coordinate system to display three-dimensional motion in space. The transformation from head-coincident coordinates to earth-fixed coordinates was given by the 3-by-3 matrix S listed in the next paragraph.

Computations by a laws-of-motion-based perfect processor of acceleration information were implemented by a system of 18 differential equations describing the processor's perceived motion and orientation, using nine 3-vectors and the matrix S :

${}^h\vec{i}_E, {}^h\vec{j}_E$ and ${}^h\vec{k}_e$: the earth's \vec{i}, \vec{j} , and \vec{k} vectors (unit x -, y -, and z -directed vectors) in head-coincident coordinates,

S : 3-by-3 matrix whose rows, in order, were ${}^h\vec{i}_E, {}^h\vec{j}_E$ and ${}^h\vec{k}_e$,

${}^h\vec{\omega}$: angular velocity, in head-coincident coordinates,

\vec{r} : center of the head coordinate system, in earth-fixed coordinates,

${}^E\vec{v}$: linear velocity, in earth-fixed coordinates,

${}^h\vec{\alpha}$: angular acceleration, in head-coincident coordinates,

${}^h\vec{A}$: gravito-inertial acceleration (GIA), in head-coincident coordinates,

${}^E\vec{g}$: vector with x and y components zero and z component $g = 9.81 \text{ m/s}^2$, or 0 m/s^2 for the MICROGRAVITY condition, representing the "pseudo-acceleration" indistinguishable from earth-upward acceleration, by Einstein's Equivalence Principle, due to the presence of gravity.

The system of differential equations, written in vector notation, was

$$\frac{d{}^h\vec{i}_E}{dt} = {}^h\vec{i}_E \times {}^h\vec{\omega}$$

$$\frac{d{}^h\vec{j}_E}{dt} = {}^h\vec{j}_E \times {}^h\vec{\omega}$$

$$\frac{d{}^h\vec{k}_E}{dt} = {}^h\vec{k}_E \times {}^h\vec{\omega}$$

$$\frac{d\vec{r}}{dt} = {}^E\vec{v}$$

$$\frac{d{}^h\vec{\omega}}{dt} = {}^h\vec{\alpha}$$

$$\frac{d{}^E\vec{v}}{dt} = S{}^h\vec{A} - {}^E\vec{g}$$

where, again, the perfect processor's assumption of the influence of gravity, ${}^E\vec{g}$, is zero for the MICROGRAVITY condition. The nine $\vec{i} - \vec{j} - \vec{k}$ equations include redundancy (e.g. \vec{k} is $\vec{i} \times \vec{j}$) to allow cross-checking in order to improve precision of the computations during rotation.

Computations with time constants were implemented by a modified system of 18 differential equations using the time constants τ_a, τ_l , and τ_t , respec-

tively, for the angular, linear, and tilt time constants:

$$\frac{d^h \vec{i}_E}{dt} = {}^h \vec{i}_E \times \left({}^h \vec{\omega} + \frac{\beta}{\tau_t} \vec{u} \right)$$

$$\frac{d^h \vec{j}_E}{dt} = {}^h \vec{j}_E \times \left({}^h \vec{\omega} + \frac{\beta}{\tau_t} \vec{u} \right)$$

$$\frac{d^h \vec{k}_E}{dt} = {}^h \vec{k}_E \times \left({}^h \vec{\omega} + \frac{\beta}{\tau_t} \vec{u} \right)$$

$$\frac{d^E \vec{r}}{dt} = {}^E \vec{v}$$

$$\frac{d^h \vec{\omega}}{dt} = {}^h \vec{\alpha} - \frac{1}{\tau_a} {}^h \vec{\omega}$$

$$\frac{d^E \vec{v}}{dt} = S^h \vec{A} - {}^E \vec{g} - \frac{1}{\tau_\ell} {}^E \vec{v}$$

where

$$\beta = \cos^{-1} \left(\frac{{}^h \vec{A} \cdot {}^h \vec{k}_E}{\|{}^h \vec{A}\|} \right)$$

is the magnitude of the angle by which the current perceived vertical differs from the direction of the GIA, and

$$\vec{u} = \frac{{}^h \vec{A} \times {}^h \vec{k}_E}{\|{}^h \vec{A} \times {}^h \vec{k}_E\|}$$

is a unit vector in the direction in which angular velocity is required in order to re-interpret vertical as being in alignment with the GIA.

The above systems of differential equations were used for all of the conditions (STANDARD, ACCELERATING, DECELERATING, MICROGRAVITY, SHORT&SLOW, LONG&SLOW, SHORT&FAST, and for other roll radii and rotation speeds); however, the accelerations ${}^h \vec{A}$ and ${}^h \vec{\alpha}$, as detected at the head, differed from one condition to the next. In order to compute these accelerations, the rightward head roll of 30° in 1s was written as a function $\theta(t)$, for which $\theta = 0$ represents upright:

$$\theta(t) = 0.2618(1 - \cos(\pi t)) \text{ for } 0 \leq t \leq 1,$$

where $0.2618 = \frac{1}{2} (0.5236 \text{ rad}) = \frac{1}{2} (30^\circ)$. Writing

$$\Omega(t) = \text{angular velocity of rotating chair, in rad/s,}$$

$$= 1 + 0.26t \text{ for ACCELERATING,}$$

$$= 1 - 0.26t \text{ for DECELERATING,}$$

$$= 1 \text{ for all other except FAST conditions,}$$

and dots for derivatives, the x -, y -, and z - components of ${}^h \vec{\alpha}$ were

$${}^h \alpha_x = \ddot{\theta}$$

$${}^h \alpha_y = \Omega \dot{\theta} \cos \theta + \dot{\Omega} \sin \theta$$

$${}^h \alpha_z = -\Omega \dot{\theta} \sin \theta + \dot{\Omega} \cos \theta$$

(which are functions of time), where the first terms in the expressions for ${}^h \alpha_y$ and ${}^h \alpha_z$ were due to cross-coupling of the earth-vertical-axis and head- x -axis angular velocities, and the second term (which is nonzero only for ACCELERATING and DECELERATING) was due to vertical-axis acceleration. The x -, y -, and z -components of ${}^h \vec{A}$ were

$${}^h A_x = 0$$

$${}^h A_y = g \sin \theta$$

$${}^h A_z = g \cos \theta$$

for the three conditions STANDARD, ACCELERATING, and DECELERATING; similarly, ${}^h A_x = {}^h A_y = {}^h A_z = 0$ for MICROGRAVITY. However, for all conditions with a nonzero roll radius r ,

$${}^h A_x = 2r\Omega \dot{\theta} \cos \theta$$

$${}^h A_y = r\Omega^2 \sin \theta \cos \theta - r\ddot{\theta} + g \sin \theta$$

$${}^h A_z = -r\Omega^2 \sin^2 \theta - r\ddot{\theta} + g \cos \theta$$

and these equations were used for conditions SHORT&SLOW, LONG&SLOW, SHORT&FAST, and for other roll radii and rotation speeds. The ${}^h A_x$ expression was tangential acceleration associated with the linear coriolis force. The first terms in the expressions for ${}^h A_y$ and ${}^h A_z$ were centripetal acceleration from the vertical-axis rotation. The second terms were due to head roll: tangential acceleration for ${}^h A_y$, and centripetal acceleration for ${}^h A_z$.

Initial conditions for each system of differential equations were made to match the initial perceptual conditions of a typical subject immediately preceding head roll. The orientation was upright, formalized by

$${}^h \vec{i}_E = \begin{bmatrix} 1 \\ 0 \\ 0 \end{bmatrix}, \quad {}^h \vec{j}_E = \begin{bmatrix} 0 \\ 1 \\ 0 \end{bmatrix}, \quad {}^h \vec{k}_E = \begin{bmatrix} 0 \\ 0 \\ 1 \end{bmatrix}.$$

In addition, most conditions were initialized with ${}^h \vec{\omega}$ and ${}^E \vec{v}$ being zero, representing no perceived angular or linear velocity while the chair is rotating at a constant speed, before the head moves. The exceptions were ACCELERATING and DECELERATING, in which subjects typically report perceived chair rotation. For those two cases, ${}^h \omega_z$ was initialized to 0.91 rad/s for ACCELERATING, and -0.91 rad/s for DECELERATING, based upon a prior 3.846 (= 1/0.26) sec acceleration or deceleration at 0.26 rad/s² and angular time constant of 20 s.

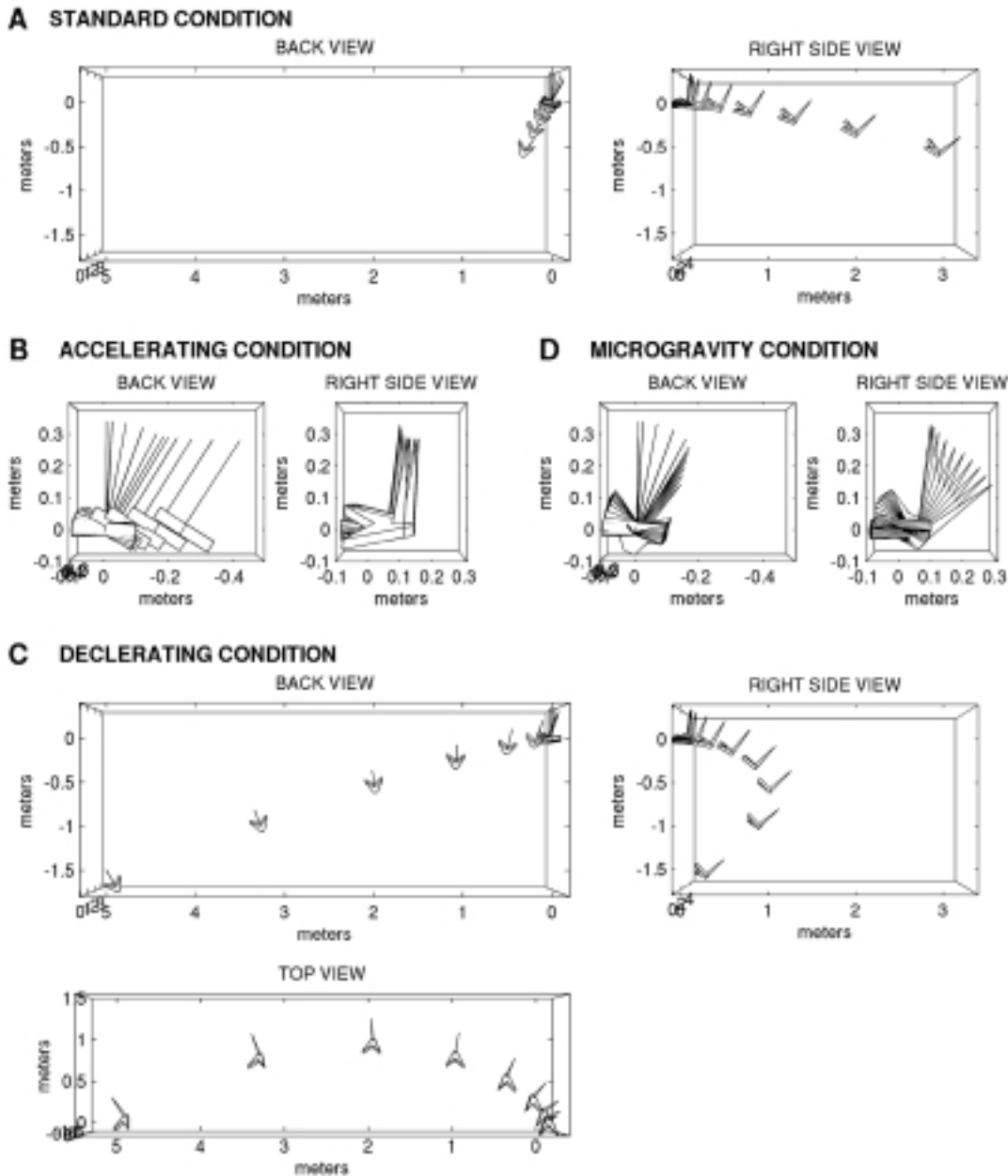


Fig. 3. Time-lapse pictures of perceived motion by the perfect processor, for 2 s, head shown every 0.2 s. The head starts at the origin (0,0,0) in each part. (A) STANDARD condition. The head proceeds forward, pitching downward. The axis ranges and scale are set for direct comparison with part (C) and Fig. 5. (B) ACCELERATING condition. The head rolls rightward with small rightward translation. The axis ranges and scale are set for direct comparison with part (D). (C) DECELERATING condition. The head proceeds forward and leftward, curving also downward and eventually backward, while pitching forward and rolling first rightward then leftward. The axis ranges and scale are set for direct comparison with part (A) and Fig. 5. (D) MICROGRAVITY condition. The head pitches forward while rolling rightward. The axis ranges and scale are set for direct comparison with part (B).

2.6. Software and hardware

The computational and graphics software were developed in Matlab (MathWorks, Inc., Natick, Mas-

sachusetts, USA), and the computations were performed on a Silicon Graphics Workstation and a Power Mac. The systems of differential equations were solved using the Runge-Kutta 45 algorithm with absolute tol-

erance 10^{-6} and relative tolerance 10^{-3} , while the \vec{i}, \vec{j} , and \vec{k} vectors were kept orthonormal by re-normalizing at each graphed time step of 0.2 s, using the Gram-Schmidt method of orthonormalization. The three-dimensional graphics were created by implementing z -buffering to handle the complexity of the overlapping three-dimensional figures.

3. Results

3.1. Conditions with on-axis head roll

Three-dimensional simulations resulted in displays of perceived motions (Fig. 3) that would be reported by a laws-of-motion-based perfect processor of acceleration information in the first set of conditions: STANDARD, ACCELERATING, DECELERATING, and MICROGRAVITY. The STANDARD condition resulted in perceived linear motion forward, in addition to perceived pitch motion forward along with the rightward roll (Fig. 3(A)). The ACCELERATING condition resulted in very little perceived linear movement, rightward, and the perceived angular motion was essentially only the actual roll motion (Fig. 3(B)). The DECELERATING condition resulted in perceived linear motion in a leftward/downward/forward-then-backward curve, in addition to perceived pitch motion forward along with rightward roll which switches to leftward roll (Fig. 3(C)). The MICROGRAVITY condition resulted in no perceived linear motion, but perceived pitch motion forward along with the rightward roll (Fig. 3(D)).

Calculations of Twist and Stretch Factors in the four conditions showed the progression of angular and linear deviations from the actual rightward head roll (Fig. 4). In the STANDARD condition, both the Twist and Stretch Factors increased continuously. In the ACCELERATING condition, neither increased substantially. In the DECELERATING condition, both increased, at approximately twice the rate as for the STANDARD condition. In the MICROGRAVITY condition, only the Twist Factor increased; the Stretch Factor remained zero throughout.

Simulations with time constants resulted in three-dimensional displays of perceived motions as reported by a processor with built-in decays of angular and linear motion perception and tendency to interpret the GIA as vertical. The perceived motions were the same shape as, but smaller magnitude than, the motions reported by a perfect processor (Fig. 3), as illustrated by the

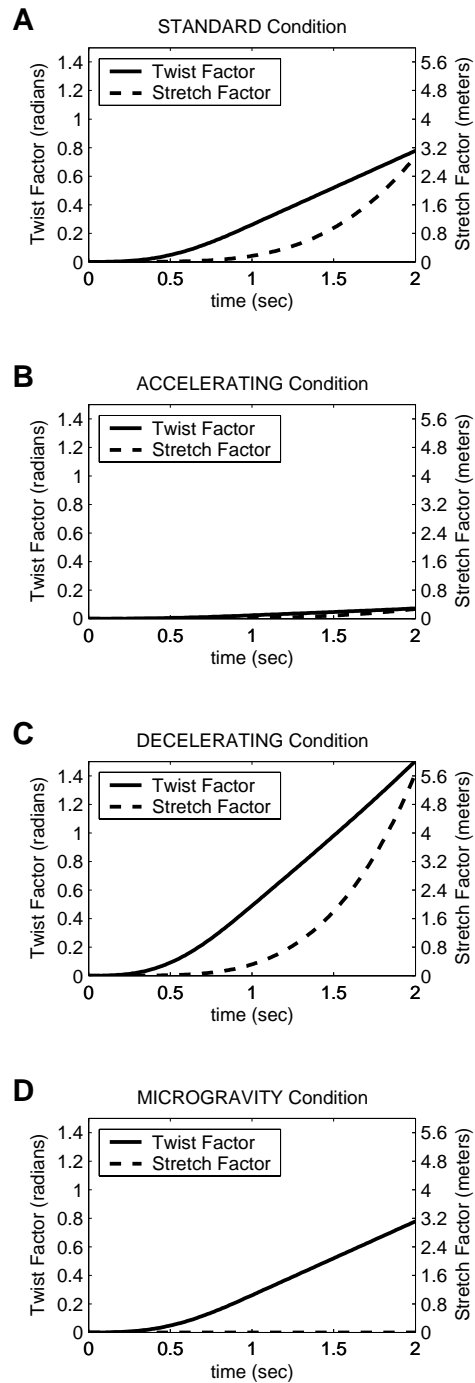


Fig. 4. Twist and Stretch Factors of perceived motion by the perfect processor. (A) STANDARD condition, corresponding to perceived motion shown in Fig. 3(A). (B) ACCELERATING condition, corresponding to Fig. 3(B). (C) DECELERATING condition, corresponding to Fig. 3(C). (D) MICROGRAVITY condition, corresponding to Fig. 3(D).

STANDARD condition (Fig. 5). Other conditions were

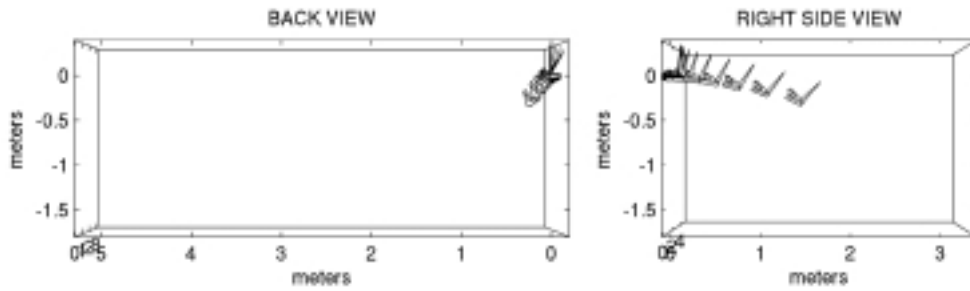


Fig. 5. With time constants included in the model, time-lapse picture of perceived motion for the STANDARD condition, for 2 s, head shown every 0.2 s. The head starts at the origin (0,0,0) and proceeds forward while pitching downward, in the same manner as, but with smaller extent of motion than, in the simulation without time constants (Fig. 3(A)). The axis ranges and scale are set for direct comparison with Fig. 3(A) and (C).

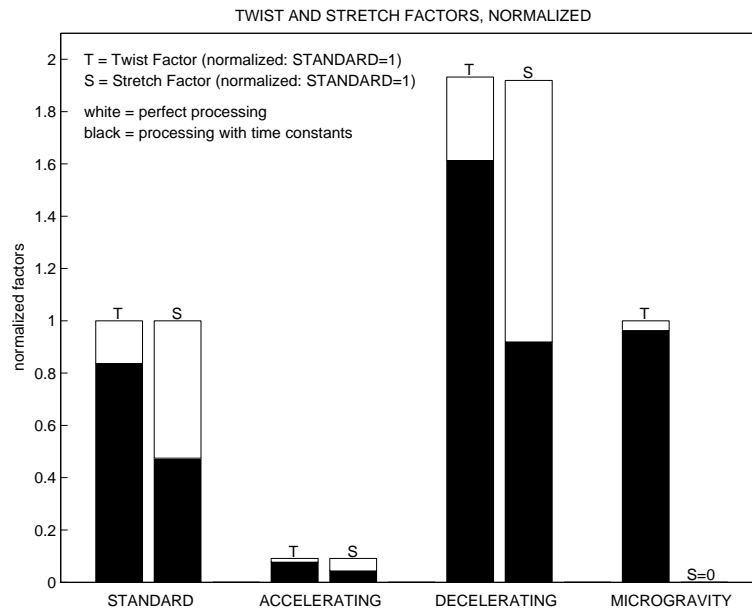


Fig. 6. Comparison of Twist and Stretch Factors at the end of 2 s, for the first set of conditions. The factors are normalized to each equal 1 in the STANDARD condition for ease of comparison. In the ACCELERATING condition, the Twist and Stretch Factors are lower by a coincidentally similar amount when perfect processing is used. In the DECELERATING condition, the Twist and Stretch Factors are higher by a coincidentally similar amount when perfect processing is used. In the MICROGRAVITY condition, the normalized Twist Factor is 1 when perfect processing is used, and the Stretch Factor is 0.

also similar to their counterparts in Fig. 3.

The Twist and Stretch Factors at the end of two seconds were computed for all simulations (Fig. 6). A comparison shows that the ACCELERATING condition had much smaller Twist and Stretch Factors than did the STANDARD condition, while the DECELERATING condition had much larger Twist and Stretch Factors.

The MICROGRAVITY condition was slightly more complicated in comparison to the STANDARD condition. First, the Twist Factors were identical in the perfect-processor simulations. However, the MICROGRAVITY condition had a slightly larger Twist Factor

than did the STANDARD condition for the simulation with time constants. This was due to the absence of gravity, which in the STANDARD condition slowed the misperception of pitch because of the tendency to interpret the GIA as vertical.

Second, the Stretch Factors were completely different between the STANDARD and MICROGRAVITY conditions, with the MICROGRAVITY condition having significantly smaller (in fact, zero) Stretch Factor. In this way, the Stretch Factor reflects the experimental results of significantly less perceptual disturbance during cross-coupling movements in microgravity. In

other words, the Stretch Factor can explain what the Twist Factor alone cannot.

3.2. Conditions with head roll to off-axis

To further investigate the Twist and Stretch Factors, simulations were carried out for conditions with rightward head roll to off-axis (i.e. moving away from the vertical axis): SHORT&SLOW, LONG&SLOW, SHORT&FAST.

Three-dimensional simulations resulted in displays of perceived motions, as reported by a laws-of-motion-based perfect processor of acceleration information (Fig. 7). The SHORT&SLOW condition (Fig. 7(A)) gave a result similar to that for the STANDARD condition (Fig. 3(A)): perceived linear motion forward, in addition to perceived pitch motion forward along with the rightward roll. The LONG&SLOW condition resulted in a very similar perceived motion (Fig. 7(B)). The SHORT&FAST condition resulted in greater perceived linear motion forward, with greater forward pitch motion along with the rightward roll (Fig. 7(C)).

The Twist and Stretch Factors at the end of two seconds were computed for all of these simulations, and for simulations with time constants (Fig. 8). The Twist and Stretch Factors were similar between the SHORT&SLOW and LONG&SLOW conditions, while the SHORT&FAST condition had significantly greater Twist and Stretch Factors, both. The difference between Twist Factors is not surprising.

Striking, though, is the comparison of Stretch Factors. The SHORT&FAST condition, which had a short neck length, resulted in a much greater Stretch Factor than did the LONG&SLOW condition, which had a longer neck length. At the same time, the LONG&SLOW condition had only a slightly greater Stretch Factor than did the SHORT&SLOW condition, even though the actual linear movement was approximately twice as great in the LONG&SLOW condition.

The Stretch Factor, therefore, reflects the experimental results of significantly greater perceptual disturbance during fast rotation than during slower rotation with a larger linear movement away from the axis. For these conditions, the Twist Factor could also explain the experimental results.

3.3. Rotation speed versus neck length

Twist and Stretch Factors were computed for the same movement but with different rotation speeds and neck lengths. The basic condition was SHORT&SL-

OW, with rotation speed of 1 rad/s and neck length of 0.1 m. A comparison was made of increased rotation speeds versus increased neck lengths. Rotation speeds of 1 rad/s, 2 rad/s, . . . 7 rad/s were used, each with neck length 0.1 m. Neck lengths of 0.1 m, 0.2 m, . . . , 0.7 m were used, each with rotation speed 1 rad/s.

Twist and Stretch Factors after two seconds were computed from simulations of perceived motions as reported by a perfect processor of acceleration information. The results (Fig. 9) show that Twist and Stretch Factors increase with increasing rotation speeds, but do not increase substantially with increasing neck lengths. For the Twist Factor, these results are not surprising.

However, for the Stretch Factor these results confirm the surprising result above for LONG&SLOW and SHORT&FAST, that the Stretch Factor is only affected slightly by neck length, but is affected significantly by rotation speed.

4. Discussion

Differences in magnitude of vestibular coriolis/cross-coupling effects are explained here in a common framework: the three-dimensional laws of motion, including all three-dimensional linear-angular interactions. In contrast to the traditional description involving angular vectors alone, the present research uses a laws-of-motion-based perfect processor of acceleration information that also takes into account all linear accelerations in three dimensions. In this way, the results show how even a perfect processor of three-dimensional acceleration information would experience perceptual disturbances of different magnitudes due to linear-angular interactions during vestibular cross-coupling in different conditions. In particular, compared to the standard constant-velocity rotation condition, an accelerating rotation is predicted to produce a much weaker effect, and a decelerating rotation is predicted to produce a much stronger effect. Compared to a 1 g environment, a zero-g environment is predicted to produce a weaker effect, despite the fact that the magnitude of the cross-coupled vectors are identical. Compared to a movement with a short "neck length" (radius of head roll), a movement with a long neck length is predicted to produce a similar-magnitude effect, while a movement with a short neck length but during faster rotation is predicted to produce a greater effect. All of these results are obtained by considering the Twist and Stretch Factors, which measure the disorienting angular and linear components, respectively, in the three-dimensional

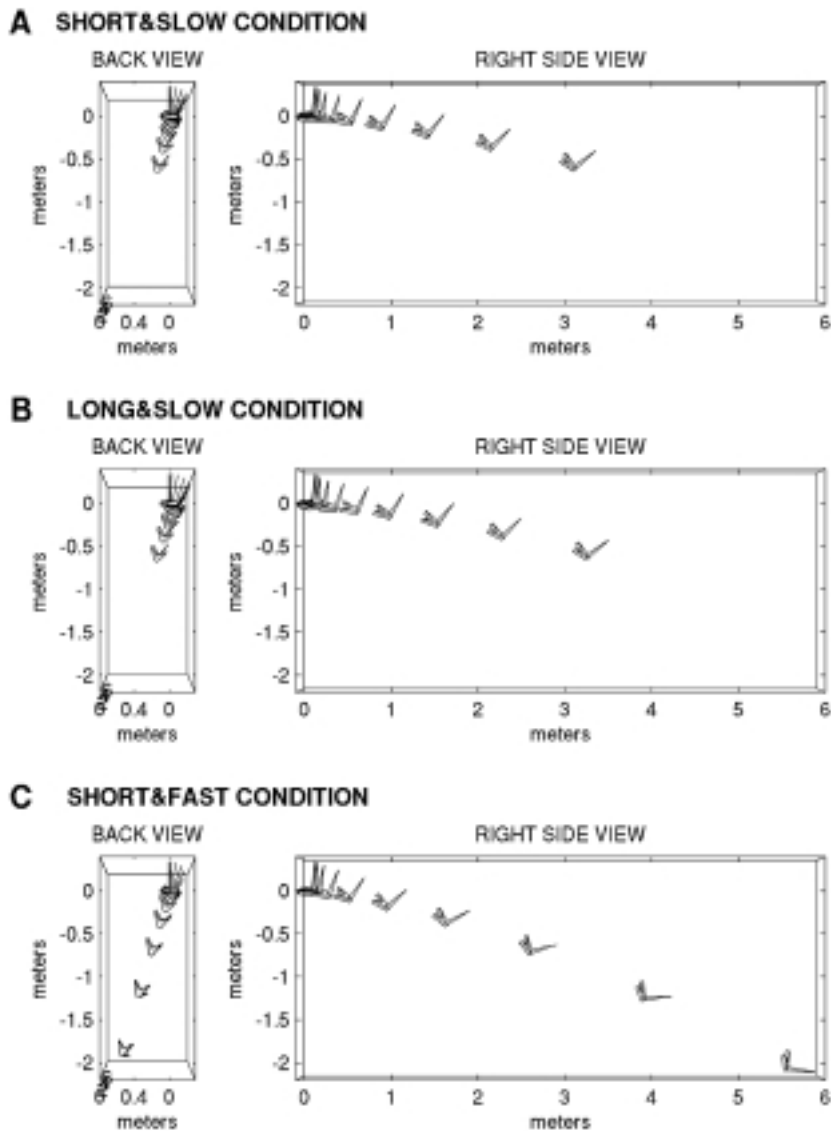


Fig. 7. Time-lapse picture of perceived motion by the perfect processor, for 2 s, head shown every 0.2 s. The head starts at the origin (0,0,0), and the axis ranges and scale are the same in all parts. (A) SHORT&SLOW condition. The head proceeds forward, pitching downward. (B) LONG&SLOW condition. The head proceeds forward, pitching downward, similar to the SHORT&SLOW condition. (C) SHORT&FAST condition. The head proceeds forward, pitching downward, with greater pitch angle and greater translational movement than in the SHORT&SLOW condition.

perceived motion as computed by the laws-of-motion-based perfect processor of acceleration information. Inclusion of linear components was found to be crucial, as the Stretch Factor was a predictor consistent with known experimental findings for all of the motions, while the Twist Factor was not as good a predictor alone. The results also hold for a model with time constants for decay of angular motion perception, for decay of linear motion perception, and for tilt so that the subjective vertical approaches alignment with the

GIA.

4.1. Comparison with experimental results

The results on accelerating and decelerating rotation conditions are consistent with experimental findings, and give a three-dimensional explanation for the findings. Experimentally [23], subjects report much weaker perceptual effects if the rotating chair is accelerating than if the chair is rotating at constant veloc-

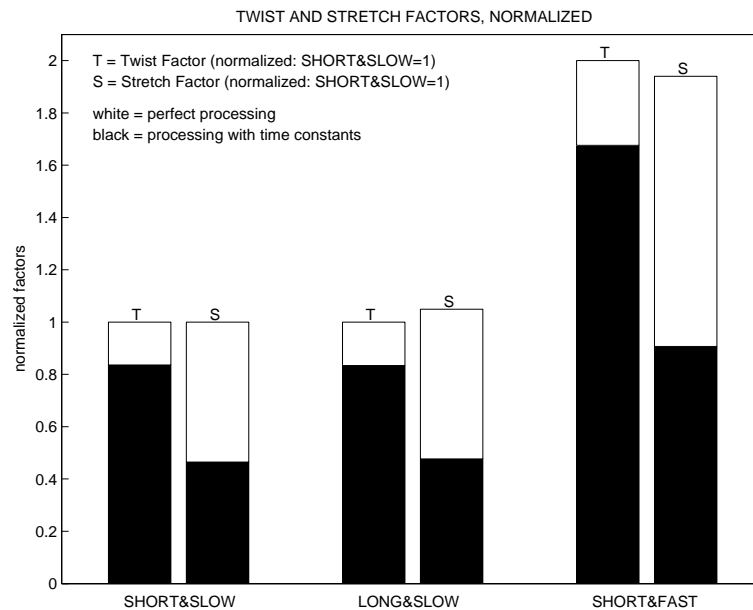


Fig. 8. Comparison of Twist and Stretch Factors at the end of 2 s, for the second set of conditions. The factors are normalized to each equal 1 in the SHORT&SLOW condition for ease of comparison. The Twist and Stretch Factors in the LONG&SLOW condition are similar to those in the SHORT&SLOW condition. The Twist and Stretch Factors are both approximately doubled in the SHORT&FAST condition.

ity. Also, subjects report much stronger perceptual effects if the rotating chair is decelerating. The experiments used the same parameters as used in the model here, with head movement lasting approximating 1 s and chair rotation speed of 1 rad/s, and with acceleration and deceleration magnitudes of 0.26 rad/s^2 . One explanation for the experimental findings [23] points to the compatibility during the accelerating condition of the gravity vector and the total semicircular-canal-based angular vector, by an alignment that occurs in everyday motions. During the decelerating condition, in contrast, the total semicircular-canal-based angular vector and the gravity vector are oriented out of alignment, and the gravity vector does not rotate in a way that would be compatible with the angular vector for typical everyday motion. Compatibility between angular and gravity vectors is thought to be a factor in the vestibular coriolis effect [5,23,35,36,57]. The present investigation quantitatively confirms such previous explanations by bringing to light the three-dimensional consequences of all vector interactions, including the alignment, misalignment, and compatibility of the angular and gravity vectors. In particular, the misalignment of the angular and gravity vectors without concurrent gravity direction change in the decelerating condition leads to the greatest Stretch Factor of all the conditions, indicating the greatest mismatch between perceived motion and actual head motion relative to the

body. In addition, the Twist Factor shows the greatest angular cross-coupling in the decelerating condition.

The results on the zero-g condition are also consistent with experimental findings, and give an explanation involving the Stretch Factor. Experimentally, subjects report much weaker perceptual effects during cross-coupling movements in zero-g [19,20,36]. The classical angular explanation of the cross-coupling effect fails to explain the differences between zero-g and 1 g because the cross-coupled angular vector is the same in both cases. Linear-angular interaction has been suggested, hence, as a factor [5,57], as has the resulting muscle activity [13,35,36]. The present modeling investigation shows that linear-angular interaction, indeed, can explain the differences between zero-g and 1 g. The three-dimensional display shows that the presence of gravity introduces a linear component of motion into the laws-of-motion computation of perceived motion, and that a substantial Stretch Factor arises in the 1 g condition. The Stretch Factor can explain why perceptual disturbances are greater in 1 g. This result does not mean that a human subject would necessarily perceive linear motion. For one thing, the subject has no proprioceptive cues to indicate that the rest of the body is being accelerated. Therefore, instead of perceiving whole-body linear motion, the subject may experience a perceptual disturbance due to a mismatch between vestibular-based processing (saying “linear mo-

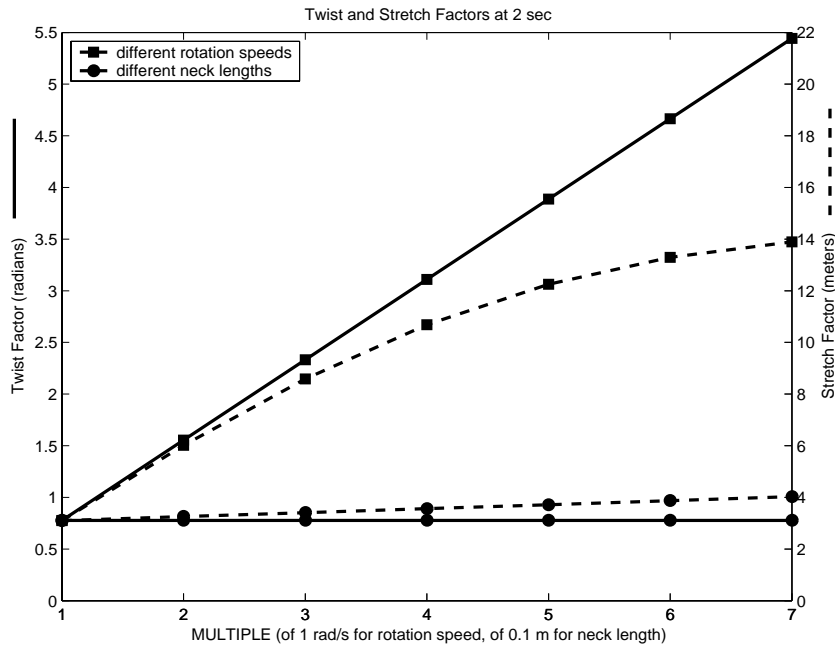


Fig. 9. Comparison: Increase in rotation speed versus increase in neck length. Both the Twist Factor and the Stretch Factor are compared. The leftmost data point corresponds to 1 rad/s rotation and 0.1 m neck length. For the “different rotation speeds” curves, a fixed neck length of 0.1 m was used. For the “different neck lengths” curves, a fixed rotation speed of 1 rad/s was used.

tion”) and body and neck proprioceptive cues (saying “no linear motion”). This concept is formalized here as the Stretch Factor.

The linear component of the three-dimensional display is therefore crucial in explaining certain differences between conditions, a fact that led in the present study to the investigation of conditions with a nonzero neck length, which leads to linear coriolis accelerations. The results here are consistent with experimental findings, and show surprisingly that the Stretch Factor is more correlated with rotation speed than with linear coriolis magnitude. Correspondingly, in experiments [32,33], subjects reported nauseogenic effects proportional to the cross-coupled angular magnitude, not to the linear coriolis magnitude. In these experiments, different radii were used for head tilt forward, with just the neck (0.1 m) or the upper body (~ 0.6 – 0.9 m) [32], or with side-to-side movement while in a forward-leaning position, with different amounts of lean to produce different magnitudes of linear coriolis acceleration [33], and at different rotation rates in the range $60^\circ/\text{s}$ to $180^\circ/\text{s}$. Both sets of experiments showed that for perceptual disturbance, the magnitude of the cross-coupled angular vector was the important parameter, not the linear coriolis acceleration. The present modeling work shows that both the Twist and Stretch Factors can explain this experimental finding. Both the

Twist and Stretch Factors are significantly greater when the cross-coupled angular vector is greater due to faster rotation speed, but are not significantly greater when the linear coriolis acceleration is greater due to a longer “neck”.

The Stretch Factor’s correlation with rotation speed can be understood, once again, as caused by linear-angular interaction. With a greater rotation speed, the cross-coupled angular acceleration is greater, causing faster perceived pitch motion. Perceived pitch motion includes an associated reorientation of the perceived vertical, while the actual gravity vector stays aligned with the body. In summary, faster rotation causes faster perceived pitch which causes the perceived vertical to move more quickly out of alignment with the GIA. From a laws-of-motion point of view, the resulting perception must then include linear acceleration as the difference between the GIA and the subjective gravity vector, because the GIA is necessarily interpreted as the sum of the gravity vector and linear acceleration. By these means, faster rotation causes greater perceived linear motion, i.e. a greater Stretch Factor.

At the same time, this three-dimensional modeling demonstrates that the Stretch Factor is not influenced substantially by the linear coriolis acceleration. Through the three-dimensional display and the computation of the Stretch Factor, it is clear that the GIA-

vertical misalignment related to rotation speed is much more important than is linear coriolis acceleration.

4.2. Models

There are similarities and differences between the present model and other three-dimensional models [2,3,6,8,14,17,34,39–41,43–45,48,50–52,56,59]. The similarities arise, as expected, from the fact that the models are modeling similar phenomena. The main differences stem from the present goals: to investigate *perception* specifically, and in a three-dimensional manner that includes *position and orientation relative to the surroundings*.

One similarity is in the computations that mirror the laws of motion, such as when modeling the noncommutativity of rotation or the interaction between angular and linear vectors to determine the direction of vertical. Because the nervous system does such a good job fundamentally dealing with angular and linear vectors, models typically find that the laws-of-motion computations are an appropriate component.

A difference, however, is that other models also include physiological dynamics as an integral part, while the present model instead aims to determine whether certain phenomena can be explained more basically by the laws of motion. The present model is designed specifically to investigate three-dimensional complex motions where the laws-of-motion results would not necessarily be intuitive. The simulation time frame is intentionally kept short so that known long-term physiological effects like canal decays do not have a substantial influence on the predicted responses; such effects would demonstrate their influence over longer time frames. The present model can determine whether even a perfect processor of acceleration information would be disoriented under the given circumstances, and can demonstrate through the laws of motion that the complicated conditions in different motions could lead to potential differences in perceptions. For example, previous work using this approach [29] showed faster change in tilt perception during deceleration than during acceleration in a fixed-carriage centrifuge, a perceptual phenomena that has also been predicted with models that include physiological parameters [8,16,17,39,40,43,52,59]. The present modeling approach showed that the centrifuge perceptual asymmetry could be explained more basically by the laws of motion.

As a consequence of the different goals of this and other models, the input and output variables are somewhat different. The present model has input GIA and

angular *acceleration* (included also in models [6,34,50]), i.e. the actual stimuli to the sensors, while most models use GIA (and linear velocity if vision is included) and angular *velocity* which is approximated by the semicircular canal afferents for certain frequencies. This is an example in which other models implicitly incorporate a sub-model of physiological dynamics. For output, the present model and other models include linear and angular velocities and the direction of gravity. The difference is that the present model also continuously computes and outputs the three-dimensional position (\vec{r}) and orientation ($\vec{i}, \vec{j}, \vec{k}$) relative to the surroundings. These vectors are necessary for a full three-dimensional perception, as displayed here by three-dimensional plots of motion, another difference between this and other models. Additionally introduced here are the Twist and Stretch Factors, made possible by the continuous processing of three-dimensional position and orientation.

A similarity with certain other models arises from the fact that the laws of motion naturally keep track of values of the variables, including the linear acceleration and the gravity vector, which must sum to the GIA. Portions of a model that keep track of and manipulate variables in this way have been termed “internal models” [2,3,8,17,39–41,43,44,52,59]. The present investigation is thus consistent with the internal-model concept.

A variation of the present model includes time constants for additional simulations to verify the results for a more human-like perceptual processor. This addition of time constants makes this aspect of the model more like other three-dimensional models, though many other models are more finely-tuned to experimental results because they model the vestibulo-ocular reflex rather than perception. The main time constants used for the present model were 20 s for decay of angular motion perception, 0.5 s for decay of linear motion perception, and 5 s for tilt to reorient the subjective vertical toward the GIA. Further testing of the present model showed that the exact values of these time constants were not important for the present goals, with time constants tested in the ranges 10–20 s for angular, 0.5–5 s for linear, and 2–5 s for tilt. These values are within experimentally determined ranges, but variation has been found experimentally. For example, rotations in the directions of the vertical canals have been found to have a shorter perceptual time constant than for horizontal rotation [25], and the angular time constant has been shown to depend on radius of rotation [46]. The time constant for tilt depends upon the experimental

set-up, especially when rotation is present [9,10,15,16, 55]. In addition, linear motion perception is strongly influenced by extra-vestibular cues, and studies show variability, often leading to a longer time constant [37, 58], while a study on a noiseless, vibrationless linear sled riding on air bearings showed that linear motion perception extinguished rapidly after the acceleration ended [54], which can be modeled by a small time constant such as used here.

4.3. Perception

Perception of complex motion is difficult for subjects to report experimentally, and even perception of simple motions can vary between subjects. For this reason, the present investigation has been aimed to produce results that hold regardless of particular subjects' specific reports of perceived motion. The concept of "perceptual disturbance" encompasses a number of phenomena such as motion sickness (as modeled, e.g., in [5,7,47]), misperception of motion, disorientation, and dizziness. The present approach is compatible with previous hypotheses for motion sickness, of sensory conflict, or of conflict between vectors as sensed and vectors as computed by an internal model, in general [47], or for the vertical vector [5,7]. The present investigation focuses on motions in which the head moves relative to the body, and extracts two measures from a three-dimensional display, the Twist Factor and the Stretch Factor, which could be interpreted as indicating either predicted perceived motion or vestibular-proprioceptive mismatch, a mismatch that could alternatively be phrased as a conflict between sensory input and estimates by an internal model. The Twist and Stretch Factors may be manifest differently in different subjects, in terms of the types of perceptual disturbances.

A further direction of research would look at the issue of active versus passive movements. In the present work, all movements were treated in the same way.

4.4. Conclusion

Linear-angular interaction is a crucial factor in three-dimensional perception and misperception of motion. Even angular-only motions produce a linear-angular interaction with gravity, such as during the vestibular cross-coupling/coriolis effect. For this reason, a complete investigation of perception necessarily involves all linear and angular components in three dimensions, as well as all interactions between the components. Modeling is becoming an increasingly integral part of research on perception as the motions studied experimentally become increasingly complicated.

Acknowledgements

Thanks to John Kuehne and Sarah Pierce for computer support and assistance. This work was funded by grants from the Colby College Division of Natural Sciences and by the Clare Boothe Luce Fund administered by the Henry Luce Foundation.

References

- [1] D. Angelaki and B.J.M. Hess, Inertial representation of angular motion in the vestibular system of rhesus monkeys. I. Vestibulo-ocular reflex, *J. Neurophysiol.* **71** (1994), 1222–1249.
- [2] D.E. Angelaki, D.M. Merfeld and B.J.M. Hess, Low-frequency otolith and semicircular canal interactions after canal inactivation, *Experimental Brain Research* **132** (2000), 539–549.
- [3] D.E. Angelaki, M. Wei and D.M. Merfeld, Vestibular discrimination of gravity and translational acceleration, *Annals of the New York Academy of Sciences* **942** (2001), 114–127.
- [4] J. Baker, J. Goldberg, G. Hermann and B. Peterson, Spatial and temporal response properties of secondary neurons that receive convergent input in vestibular nuclei of alert cats, *Brain Research* **294** (1984), 138–143.
- [5] W. Bles, Coriolis effects and motion sickness modelling, *Brain Research Bulletin* **47** (1998), 543–549.
- [6] J. Borah, L.R. Young and R.E. Curry, Optimal estimator model for human spatial orientation, *Annals of the New York Academy of Sciences* **545** (1988), 51–73.
- [7] J.E. Bos and W. Bles, Modelling motion sickness and subjective vertical mismatch detailed for vertical motions, *Brain Research Bulletin* **47** (1998), 537–542.
- [8] J.E. Bos and W. Bles, Theoretical considerations on canal-otolith interaction and an observer model, *Biological Cybernetics* **86** (2002), 191–207.
- [9] B. Clark and A. Graybiel, Factors contributing to the delay in the perception of the oculogravic illusion, *American Journal of Psychology* **79** (1966), 377–388.
- [10] I.S. Curthoys, The delay of the oculogravic illusion, *Brain Research Bulletin* **40** (1996), 407–412.
- [11] I.S. Curthoys and C.H. Markham, Convergence of labyrinthine influences on units in the vestibular nuclei of the cat, I. Natural stimulation, *Brain Research* **35** (1971), 469–490.
- [12] J.D. Dickman and D.E. Angelaki, Vestibular convergence patterns in vestibular nuclei neurons of alert primates, *J. Neurophysiol.* **88** (2002), 3518–3533.
- [13] P. DiZio, J.R. Lackner and J.N. Evanoff, The influence of gravito-inertial force level on oculomotor and perceptual responses to sudden stop stimulation, *Aviation, Space, and Environmental Medicine* **58** (1987), A224–A230.
- [14] J. Droulez and C. Darlot, The geometric and dynamic implications of the coherence constraints in three-dimensional sensorimotor interactions, in: *Attention and Performance*, M. Jeannerod, ed., Lawrence Erlbaum, Hillsdale, NJ, 1989, pp. 495–526.
- [15] S. Glasauer, Interaction of semicircular canals and otoliths in the processing structure of the subjective zenith, *Annals of the New York Academy of Sciences* **656** (1992), 847–849.

- [16] S. Glasauer, Human spatial orientation during centrifuge experiments: Non-linear interaction of semicircular canals and otoliths, in: *Proc. XVIIth Barany Society Meeting (Prague 1992)*, H. Krejčová and J. Jerabek, eds, 1993, pp. 48–52.
- [17] S. Glasauer and D.M. Merfeld, Modelling three-dimensional vestibular responses during complex motion stimulation, in: *Three-Dimensional Kinematics of Eye, Head and Limb Movements*, M. Fetter, T. Haslwanter, H. Misslich and D. Tweed, eds, Harwood, Reading, 1997, pp. 387–398.
- [18] A. Graybiel and R.H. Brown, The delay in visual reorientation following exposure to a change in direction of resultant force on a human centrifuge, *The Journal of General Psychology* **45** (1951), 143–150.
- [19] A. Graybiel, E.F. Miller II. and J.L. Homick, Individual differences in susceptibility to motion sickness among six Skylab astronauts, *Acta Astronautica* **2** (1975), 155–174.
- [20] A. Graybiel, E.F. Miller and J.L. Homick, Experiment M131. Human vestibular function, in: *Biomedical Results from Skylab*, (Section II), R.S. Johnston and L.F. Dietlein, eds, NASA SP-377, US. Government Printing Office, 1977, pp. 74–103.
- [21] J.J. Groen, The problems of the spinning top applied to the semi-circular canals, *Confin. neurol.* **21** (1961), 454–455.
- [22] F.E. Guedry, Jr., Psychophysics of vestibular sensation, in: *Handbook of Sensory Physiology*, (Vol. VI), H.H. Kornhuber, ed., Springer, Berlin, 1974, pp. 3–154.
- [23] F.E. Guedry, Jr. and A.J. Benson, Coriolis cross-coupling effects: disorienting and nauseogenic or not? *Aviation, Space, and Environmental Medicine* **49** (1978), 29–35.
- [24] F.E. Guedry, A.H. Rupert, B.J. McGrath and C.M. Oman, The dynamics of spatial orientation during complex and changing linear and angular acceleration, *Journal of Vestibular Research* **2** (1992), 259–283.
- [25] F.E. Guedry, Jr., C.W. Stockwell and R.D. Gilson, Comparison of subjective responses to semicircular canal stimulation produced by rotation about different axes, *Acta Otolaryng* **72** (1971), 101–106.
- [26] H. Hecht, J. Kavelaars, C.C. Cheung and L.R. Young, Orientation illusions and heart-rate changes during short-radius centrifugation, *Journal of Vestibular Research* **11** (2001), 115–127.
- [27] W.C. Hixson, J.I. Niven and M.J. Correia, *Kinematics Nomenclature for Physiological Accelerations*, Monograph 14, Pensacola, Naval Aerospace Medical Institute, Florida, 1966.
- [28] J.E. Holly, Subject-coincident coordinate systems and sustained motions, *International Journal of Theoretical Physics* **35** (1996), 445–473.
- [29] J.E. Holly, Three-dimensional baselines for perceived self-motion during acceleration and deceleration in a centrifuge, *Journal of Vestibular Research* **7** (1997), 45–61.
- [30] J.E. Holly, Baselines for three-dimensional perception of combined linear and angular self-motion with changing rotational axis, *Journal of Vestibular Research* **10** (2000), 163–178.
- [31] J.E. Holly, Perceptual disturbances predicted in zero-g through three-dimensional modeling, *Journal of Vestibular Research* **13** (2003), 173–186.
- [32] N. Isu, M. Yanagihara, T. Mikuni and J. Koo, Coriolis effects are principally caused by gyroscopic angular acceleration, *Aviation, Space, and Environmental Medicine* **65** (1994), 627–631.
- [33] N. Isu, M. Yanagihara, S. Yoneda, K. Hattori and J. Koo, The severity of nauseogenic effect of cross-coupled rotation is proportional to gyroscopic angular acceleration, *Aviation, Space, and Environmental Medicine* **67** (1996), 325–332.
- [34] K. Kushiro, M. Dai, M. Kunin, S.B. Yakushin, B. Cohen and T. Raphan, Compensatory and orienting eye movements induced by off-vertical axis rotation (OVAR) in monkeys, *Journal of Neurophysiology* **88** (2002), 2445–2462.
- [35] J.R. Lackner and P. DiZio, Multisensory, cognitive, and motor influences on human spatial orientation in weightlessness, *Journal of Vestibular Research* **3** (1993), 361–372.
- [36] J.R. Lackner and A. Graybiel, The effective intensity of coriolis, cross-coupling stimulation is gravito-inertial force dependent: implications for space motion sickness, *Aviation, Space, and Environmental Medicine* **57** (1986), 229–235.
- [37] V.V. Marlinsky, Vestibular and vestibulo-proprioceptive perception of motion in the horizontal plane in blindfolded man—I, Estimations of linear displacement, *Neuroscience* **90** (1999), 389–394.
- [38] G. Melvill Jones, Origin significance and amelioration of coriolis illusions from the semicircular canals: a non-mathematical appraisal, *Aerospace Medicine* **41** (1970), 483–490.
- [39] D.M. Merfeld, Modeling human vestibular responses during eccentric rotation and off vertical axis rotation, *Acta Otolaryngologica, Supplement* **520** (1995), 354–359.
- [40] D.M. Merfeld, Modeling the vestibulo-ocular reflex of the squirrel monkey during eccentric rotation and roll tilt, *Experimental Brain Research* **106** (1995), 123–134.
- [41] D.M. Merfeld, L.R. Young, C.M. Oman and M.J. Shelhamer, A multidimensional model of the effect of gravity on the spatial orientation of the monkey, *Journal of Vestibular Research* **3** (1993), 141–161.
- [42] D.M. Merfeld, L. Young, G. Paige and D. Tomko, Three dimensional eye movements of squirrel monkeys following postrotatory tilt, *Journal of Vestibular Research* **3** (1993), 123–139.
- [43] D.M. Merfeld and L.H. Zupan, Neural processing of gravito-inertial cues in humans, III. Modeling tilt and translation responses, *Journal of Neurophysiology* **87** (2002), 819–833.
- [44] D.M. Merfeld, L. Zupan and R.J. Peterka, Humans use internal models to estimate gravity and linear acceleration, *Nature* **398** (1999), 615–618.
- [45] T. Mergner and S. Glasauer, A simple model of vestibular canal-otolith signal fusion, *Annals of the New York Academy of Sciences* **871** (1999), 430–434.
- [46] M-L. Mittelstaedt and H. Mittelstaedt, The influence of otoliths and somatic graviceptors on angular velocity estimation, *Journal of Vestibular Research* **6** (1996), 355–366.
- [47] C.M. Oman, A heuristic mathematical model for the dynamics of sensory conflict and motion sickness, *Acta Otolaryngologica, Supplement* **392** (1982), 1–44.
- [48] C.C. Ormsby and L.R. Young, Integration of semicircular canal and otolith information for multisensory orientation stimuli, *Mathematical Biosciences* **34** (1977), 1–21.
- [49] A.A. Perachio, G.A. Bush and D.E. Angelaki, A model of responses of horizontal-canal-related vestibular nuclei neurons that respond to linear head acceleration, *Annals of the New York Academy of Sciences* **656** (1992), 795–801.
- [50] T. Raphan and B. Cohen, The vestibulo-ocular reflex in three dimensions, *Experimental Brain Research* **145** (2002), 1–27.
- [51] T. Raphan and D. Sturm, Modeling the spatiotemporal organization of velocity storage in the vestibuloocular reflex by optokinetic studies, *Journal of Neurophysiology* **66** (1991), 1410–1421.
- [52] G. Reymond, J. Droulez and A. Kemeny, Visuo-vestibular perception of self-motion modeled as a dynamic optimization process, *Biological Cybernetics* **87** (2002), 301–314.

- [53] E.J. Searles and C.D. Barnes, Ipsilateral utricular and semi-circular canal interactions from electrical stimulation of individual vestibular nerve branches recorded in the descending medial longitudinal fasciculus, *Brain Research* **125** (1977), 23–36.
- [54] S.H. Seidman, G. Bush, G.D. Paige and D.L. Tomko, Perception of translational motion in the absence of non-otolith cues, *Soc. Neurosci. Abstr.* **24**(Part 1) (1998), 416.
- [55] S.H. Seidman, L. Telford and G.D. Paige, Tilt perception during dynamic linear acceleration, *Experimental Brain Research* **119** (1998), 307–314.
- [56] S. Wearne, T. Raphan and B. Cohen, Effects of tilt of the gravito-inertial acceleration vector on the angular vestibuloocular reflex during centrifugation, *Journal of Neurophysiology* **81** (1999), 2175–2190.
- [57] L.R. Young, Perception of the body in space: mechanisms, in: *Handbook of Physiology*, (Vol. III) (Sensory Processes, Part 2), I. Darian-Smith, ed., American Physiological Society, Bethesda, Maryland, 1984, pp. 1023–1066.
- [58] L.R. Young and J.L. Meiry, A revised dynamic otolith model, *Aerospace Medicine* **39** (1968), 606–608.
- [59] L.H. Zupan, D.M. Merfeld and C. Darlot, Using sensory weighting to model the influence of canal, otolith and visual cues on spatial orientation and eye movements, *Biological Cybernetics* **86** (2002), 209–230.